

Internal Structure of Bitumen/Polymer/Wax Ternary Mixtures for Warm Mix Asphalts

Damiano Rossi,¹ Sara Filippi,¹ Filippo Merusi,² Felice Giuliani,³ Giovanni Polacco¹

¹Department of Civil and Industrial Engineering, University of Pisa, Largo Lucio Lazzarino, 1, 56126 Pisa, Italy

²Department of Physics and Earth Sciences, University of Parma, Parco Area delle Scienze, 7/A - 43124 Parma, Italy

³Department of Civil and Environmental Engineering, University of Parma, Parco Area delle Scienze, 181/A - 43124 Parma, Italy

Correspondence to: G. Polacco (E-mail: g.polacco@diccism.unipi.it)

ABSTRACT: Polymer modified asphalts (PMA) and warm mix asphalts (WMA) are technologies widely adopted in the paving industry. The first one is well established, while the second one is relatively new, but rapidly growing since it guarantees economic and environmental advantages. Until now PMA and WMA have been used disjointedly, but it would be useful to combine them to keep the advantages of both. One of the adopted solutions to obtain a warm effect is the addition of waxes to the asphaltic binder. Therefore, a “warm mix polymer modified asphalt” may be potentially obtained with a ternary asphalt/polymer/wax system. However, the final warm effect and performances of the binder will depend on the interactions between the three components. A preliminary investigation was done by mixing asphalt, styrene-butadiene-styrene block copolymer and a wax chosen among the following three categories: paraffinic, partially oxidized and maleic anhydride functionalized. The morphological and calorimetric analyses and solubility tests allowed identifying different behaviors depending on the wax type, which may preferentially interact either with the asphalt or with the polymer, thus influencing the whole binder structure. With regard to the ternary mixes, it was found that: (i) the paraffinic wax preferentially resides in the polymer-rich phase, and slightly enhances the asphalt-polymer compatibility; (ii) the partially oxidized wax prefers the asphaltene-rich phase and reduces the compatibility; (iii) it is not clear where the functionalized wax is located, but it has a considerable compatibilizing effect and strongly alters the colloidal equilibrium of the asphalt-polymer blend. © 2013 Wiley Periodicals, Inc. *J. Appl. Polym. Sci.* 129: 3341–3354, 2013

KEYWORDS: morphology; differential scanning calorimetry; microscopy

Received 27 November 2012; accepted 21 January 2013; published online 25 February 2013

DOI: 10.1002/app.39057

INTRODUCTION

General Background

Warm mix asphalt (WMA) is a terminology that indicates all technologies that allow a reduction of the temperatures traditionally used for pavements based on asphalt binders. Compared with the traditional hot mix asphalts (HMA), the main advantages of WMA are: (a) lower fuel consumption and costs; (b) lower production of greenhouse gases, fumes and odors, thus reducing the environmental impact and improving the “*in situ*” working conditions; (c) extension of the paving season; (d) extension of the haul distances; (e) good workability during laying and compaction. Even if the development of WMA began very recently (it was prompted in the late 1990s by the German Bitumen Forum and brought to the United States in 2002), today many operators consider WMA as the future of asphalts and in the last years there has been a dramatic increase of commercial processes and technologies available on the market. The main technologies that have been developed to produce WMAs are: (1) the addition of a synthetic zeolite during mixing at the plant to

create a foaming effect in the binder; (2) a two-component binder system which introduces a soft binder and a hard foamed binder at different stages during plant production; (3) the use of organic additives such as paraffin or Montan waxes.¹ The common point to all these possibilities is the reduction of the viscosity to allow the aggregate to be fully coated at temperatures lower than those traditionally required in pavement production. The main drawback is that some of these technologies require significant equipment modifications. Moreover, these technologies have still to be considered at a developing stage and need further investigation and research to validate their added value. It is important to remember that the desired goal is to have a final product with performances comparable to those of HMA, so that it is necessary to carefully evaluate how and how much the warm additives or procedures affect the binder properties at the in-service temperatures. As already stated, one of the technologies to shift from HMA to WMA is based on waxes, because above their melting temperature, they basically act as a plasticizer, while at low temperatures they crystallize and act as filler.^{2,3} Therefore,

the wax melting temperature is the key point. It has to be higher than the service temperature and low enough to facilitate the construction operations. Of course, the presence of waxes also affects the binder performances. As an example, wax melting can soften asphalt at high service temperatures, thus reducing the rutting resistance of the pavement, while the wax crystals may increase the stiffness and sensitivity to fatigue and thermal cracking at low temperatures.^{4,5} Of course, even if not artificially added, waxes may be present as natural constitutive components of all petroleum products, asphalts included.^{6,7} Thus, waxes are present in asphalt technical literature since a long time. Studies were carried out about the determination of the wax content in bitumen,^{4,8} the crystallization properties,⁹ the chemical structure^{10,11} and the influence on asphalt and asphalt mixtures properties.^{3,5,12–17}

Another well-known and widely diffused technology is the one of polymer modified asphalts (PMA) where a polymer is added to the bituminous binder to enhance its performance and durability. Not all polymers can be used as asphalt modifiers and the most important and restrictive requirement in this sense is the compatibility with asphalt.¹⁸

Even if both well-established and used in the industrial practice, WMA and PMA have been so far mainly used disjointedly and, in spite of the abundant literature available on either of these asphalt types, there is very scarce literature concerning the production of PMA compatible with the WMA requirements. However, in the last years there is an increasing interest in developing a warm polymer modified asphalt which could contemporary maintain the advantages of both technologies. This combined technology could be defined as warm mix polymer modified asphalt (WMPMA). This is not an easy task because waxes reduce the high temperature viscosity while increasing the low temperature stiffness and polymers do basically the contrary. In other words, polymer modification is somehow in contrast with the philosophy of WMAs and the simple addition of the two ingredients does not guarantee that the properties related to the presence of polymer and wax would be maintained. On the contrary, in a ternary asphalt/polymer/wax mixture the final viscoelastic properties may significantly differ from those predictable by a simple superposition of the effects related to the presence of wax and polymer. This is not surprising if we consider that asphalt is a complex colloidal structure where a metastable equilibrium derives from the interactions among all the involved components.

The scientific literature already available about these ternary mixes is quite limited and mainly dedicated to the binder or mastic performances. Edwards et al.¹⁹ studied the addition of paraffinic waxes to polymer modified mastic asphalts and concluded that using up to at least 4% of wax additive improve workability for the mastic asphalt without seriously affecting its performances. Kim et al.^{20,21} subjected to short and long-term artificial ageing a PMA blended with warm additives. Other studies are dedicated to the properties and pavement performance,²² compacting temperatures,²³ long term performances,²⁴ use of heated-reclaimed asphalt pavement and wax,²⁵ fatigue characteristics,²⁶ and thermo-mechanical properties²⁷ of asphalt

mixtures containing warm mix asphalt additives. Moreover, the effect of wax on viscosity²⁸ and rheological properties²⁹ of modified asphalt were also evaluated. However, to our knowledge the internal structure and mutual interactions among the three components has not yet been investigated and this is the main focus of this work. A good understanding of such interactions would help to appropriately design WMPMA based on the asphalt and polymer properties and characteristics.

Polymer-Modified Asphalts

PMA are complex binary systems, where the two components interact differently according to their specific structure, composition, and chemical functionalities. In PMA the polymers preferably interact with maltenes, often leading to a final morphology where a polymer-rich phase (PRP) and an asphaltene-rich phase (ARP) coexist in a microscale metastable equilibrium. PRP can be seen as a gel, mainly swollen by the lighter asphalt components, which occupies a volumetric fraction far greater than that of the polymer in the blend. The so-called “phase inversion” occurs when the polymeric phase becomes a continuum and coincides with a dramatic change of the binder properties, which markedly reflect those of the polymer. From a thermodynamic point of view, PRP and ARP will always tend to separate. Whether they do or not is mainly a kinetic condition that assumes critical importance during prolonged storage at high temperatures in the absence of mixing. However, it is important to underline that this partial solubility and compatibility are at the same time a problem and a necessity to obtain binders with good properties. The partial solubility allows the polymer to maintain its basic morphological structure, and therefore to transfer its physical characteristics and properties to the entrapped asphalt. At the same time, a certain grade of compatibility is needed to favor the swelling process and avoids phase separation during storage. The modification with a polymer is, therefore, successful only if the right balance within these two counteracting requirements is found. This explains why the compatibility is always the critical point, which strongly limits the usable polymers. In the scientific literature, a great variety of polymers have been tested as modifiers, including thermoplastic elastomers,^{30–34} plastomers,^{35–37} and reactive polymers (containing functional groups capable of forming chemical bonds with some asphalt molecules).^{38,39} However, only thermoplastic block copolymers and ethylene-vinyl acetate (EVA) copolymers found extensive application in the industrial practice.

Thermoplastic block copolymers are by far the most frequently used, and among them poly(styrene-*b*-butadiene-*b*-styrene) (SBS) is the preferred one. The morphology of SBS shows glassy styrenic domains dispersed in a butadienic soft matrix.⁴⁰ The rigid domains, interconnected through the flexible chains, constitute the nodes of a physical network, which is responsible for the elastomeric behavior and whose structure must be preserved after mixing with asphalt so that the elastic properties can be transferred to the whole mass. This means that after the mechanical dispersion of the copolymer in the molten asphalt under high shear, during cooling the styrenic blocks must reaggregate. Moreover, at least part of the polymer-incompatible asphaltenes must be driven in the olefinic phase by the resins

which act as a surfactant for the asphaltene micelles. Every alteration of the asphalt composition and asphaltene aggregation will immediately be reflected in the PMA structure and properties. Therefore, the key point is what happens after addition of waxes which may potentially redistribute and transform the asphalt structure and morphology.

Wax in Bitumen

As it is for the polymers, in the context of asphalt research and technology, waxes used for WMAs are also quite abundant and can be divided in: (i) paraffinic waxes derived from the Fischer–Tropsch process; (ii) Montan waxes and modified Montan waxes, (iii) functionalized waxes. Montan waxes are fossilized plant waxes composed of long-chain carboxylic acid esters, free long-chain organic acids, long-chain alcohols, ketones, hydrocarbons and resins. The Fischer–Tropsch waxes are probably the most commonly used, and, due to their apolar character, they are also those expected to have the lesser interactions with polymer. On the contrary, Montan and functionalized waxes may actively interact through physical and (in some cases) chemical bonding with the polymer and the most polar asphalt molecules. In this regard, a wax may potentially play a double role of warm additive and asphalt/polymer compatibilizer, thus leading to a synergistic effect of wax and polymer on bitumen performances and workability. Of course, this is the most desirable perspective, but the interactions between wax and asphaltene may also be potentially negative from the point of view of the asphalt/polymer compatibility. If and how wax and asphaltene interact is an old, and odd, question, which has been studied quite extensively,⁴¹ because they both may precipitate during recovery and transportation of oil, thus causing serious problems in pipelines and vessels. A key unresolved issue is whether they interact synergistically during precipitation. This could be considered quite improbable, since these two fractions differ the most among all oil fractions: asphaltene are the most aromatic and polar and waxes are the most aliphatic and nonpolar. Nevertheless, it is hypothesized that the intermolecular interactions of some subset of the wax molecules with the asphaltene molecules may induce coprecipitation. However, despite many years of research that has been focused on waxes and asphaltene precipitation,^{42–44} there is still neither a consensus nor a fundamental understanding of this phenomenon. Yang and Kilpatrick,⁴¹ concluded that there is no evidence for any intermolecular interaction between waxes and asphaltene to suggest synergy in precipitation, so that only one between wax and asphaltene undergoes a phase change and precipitates, while the other one is just a portion of the crude oil occluded in the deposit. In contrast, Mahmoud et al.⁴⁵ observed that mixing of *n*-alkanes with asphaltene leads to exothermic thermal effects irrespective of the asphaltene being already precipitated or dissolved. The phenomenon is attributed to a partial immobilization of *n*-alkanes in the protecting shell formed by aliphatic lateral chains of asphaltene and validates the idea that *n*-alkanes contribute to both nucleation of the wax crystals and asphaltene flocculation. At the same time, the fact that flocculated asphaltene enhance the wax crystallization process in highly paraffinic crude oils was demonstrated by Garcia,⁴⁴ who interpreted the asphaltene particles as nucleation sites able to accelerate the

wax crystal growing. Carbognani et al., showed that the elution of paraffin concentrates through solid asphaltene packed inside high-performance liquid chromatography columns was not possible due to the formation of molecular complexes composed of very long *n*-alkanes and highly aromatic asphaltene.⁴⁶ Tinsley et al.⁴⁷ examined the effects of asphaltene upon the crystallization behavior of a model waxy oil and found that both the relative amount of wax to asphaltene and the aggregation state of the asphaltene affected the crystallization properties of the wax. In the presence of large asphaltene aggregates the wax precipitation temperature increased, while at lower asphaltene concentrations and degree of aggregation, the wax precipitation was suppressed.

Not going deeper in the description of such interactions, which are out of the scope of this work, it is just important to underline that wax addition may significantly alter the colloidal structure of the asphaltic binder, which, in turn, strongly affects the modification with a polymer. And, of course, the polymer may affect the wax behavior, which is another active field of research, basically aimed at suppressing or at least reducing wax deposition in pipelines. In this respect, effective polymers usually have crystallizable domains either included in the backbone or grafted to the polymer backbone.⁴⁸ Examples are copolymers of ethylene and vinyl acetate (EVA)^{49,50} or of maleic anhydride and acrylic acid. In the latter the crystallizable segments are provided by comonomers (such as long R-olefins) and/or by reaction of the maleic anhydride/acid group with a long chain alcohol or amine.⁵⁰ Such polymers interfere with the growth of wax crystals and their ability to form interlocking networks. Although the potential effects of such polymers have long been known,⁵¹ the mechanism of their action is still a subject of study.⁵²

In summary, it is quite clear that asphalt and added modifiers of a WMPMA may actively interact and interfere one to each other, thus forming a very complex system whose behavior is unpredictable and strongly depend on the nature and composition of all the components. Nevertheless, even if the system is very complex, some general indications may be obtained to address the formulation and the industrial processing of effective WMPMA. In this study, a preliminary characterization of asphalt/wax/polymer ternary systems is attempted, with particular attention to morphological properties. The mixes were prepared by using a base asphalt (BA), a radial SBS block copolymer and three waxes having different polarity and structure.

EXPERIMENTAL

The base asphalt is a vacuum distillation asphalt, with penetration grade 50/70. Three different waxes were used. The first one is Asphaltan[®]B, by Romonta, a mixture of substances on the basis of Montan wax constituents and higher molecular weight hydrocarbons, referred in the text as M. The second one is Epolene[®] EE-2 by Westlake Chemical, a medium density, low molecular-weight oxidized polyethylene, referred in the text as PEox. The third one is Epolene[®] E25 by Westlake Chemical, a maleic anhydride grafted polypropylene, referred in the text as PPMA. With regard to M, it is important to underline that

Table I. Blends Identification and Composition

Blend identification	SBS content (%)	Wax type (-)	Wax content (%)
BA	-	-	-
BA-SBS	5.0	-	-
BA-M2	-	M	2.0
BA-M4	-	M	4.0
BA-PEox2	-	PEox	2.0
BA-PEox4	-	PEox	4.0
BA-PPMA2	-	PPMA	2.0
BA-PPMA4	-	PPMA	4.0
BA-SBS-M2	5.0	M	2.0
BA-SBS-M4	5.0	M	4.0
BA-SBS-PEox2	5.0	PEox	2.0
BA-SBS-PEox4	5.0	PEox	4.0
BA-SBS-PPMA2	5.0	PPMA	2.0
BA-SBS-PPMA4	5.0	PPMA	4.0

from an infrared spectroscopy it resulted a paraffinic wax, where, despite of the Montan origin, the presence of oxidized functional groups was not detected.⁵³

The radial SBS was Europrene[®] SOL T 161 B by Polimeri Europa, with 30% w styrene and melt flow index <1 (ASTM D 1238, 190°C, 5 kg).

The blends preparation included: (i) asphalt/wax binary blends; (ii) asphalt/SBS binary blend; (iii) asphalt/SBS/wax ternary blends. All the binary (asphalt/wax or asphalt/SBS) and ternary (asphalt/SBS/wax) blends were prepared as follows. An asphalt sample of 250 g ± 5 g was heated in a ventilate oven until it reached a temperature of 160°C ± 5°C and subsequently placed on a heating plate. Preweighted waxes and/or SBS were slowly (5 g min⁻¹) added to asphalt and subsequently mixed for 30 min with a high shear mixer (Silverson L4R) set at 5000 rpm. During the mixing phase the temperature was maintained below 180°C. Then, the samples were subjected to a 1 h digestion at low shear rate and 180°C. Finally, the obtained binders were split into appropriate amounts to prepare samples for all the subsequent characterizations.

The prepared binary and ternary formulations and respective adopted nomenclature are reported in Table I, where the content of polymer and waxes are expressed as weight % with respect to the binder.

The first part of the experimental program is dedicated to the morphological analysis of the blends. Two different techniques were used: (i) polarized optical microscopy (POM) and (ii) fluorescence microscopy (FM). POM was mainly used to study the morphological characteristics of wax crystals and was carried out by using a Leitz Ortholux microscope with Linkam TMS 93 heating plate. Samples subjected to POM analysis were previously conditioned at 160°C with a heating rate of 10°C min⁻¹, maintained at 160°C for 10 min and then cooled with a rate of 10°C min⁻¹ up to room temperature (25°C ± 1°C). To better

observe the wax crystallites, all POM images were taken 24 h after preparation of the sample.

For FM, asphalt samples taken directly from the mixing can were poured into small cylindrical molds (10 mm internal diameter, 20 mm height), preheated to the mixing temperature. The molds were put in an oven at 180°C for 15 min, cooled to room temperature and then chilled to -30°C. The cold samples were then fractured, and the fracture surfaces examined with a LEICA DM LB fluorescence microscope.

Morphological and thermal analyses were also carried out on samples subjected to high temperature storage stability. The high temperature storage stability test (tube test) was performed according to UNI-EN 13399 (3 days at 180°C). Samples subjected to storage stability tests were divided in two fractions, respectively identified as the “top” fraction and the “bottom” fraction according to the usual technical nomenclature.

Then, the subsequent experimental steps focused on thermal properties and solubility of the blends.

Thermal properties were studied by differential scanning calorimetry (DSC) performed with a Pyris 1 scanning calorimeter from Perkin Elmer, by using sealed steel pans. The sample mass was in the range of 20–30 mg. The thermal history of the samples was as follows: fast heating up to 160°C (30°C min⁻¹), isothermal for 5 min, cooling (10°C min⁻¹) to -60°C, isothermal for 5 min and subsequent heating to 160°C (10°C min⁻¹). Data were collected during the second heating. The DSC data were used to determine glass transitions, melting temperatures, and melting enthalpies.

For the solubility tests, the molten asphalt or mix was poured into cylindrical molds with internal diameter of 20 mm and capacity of about 5 cm³. Then the sample was allowed to cool to room temperature and the excess of asphalt was trimmed with a hot spatula. The specimen was conditioned at 40°C for 2 h, weighed and placed on a metallic support with the free surface on the bottom. Finally everything was dipped in kerosene jet fuel A-type at 40°C and kept immersed for 2 h. After immersion, the specimen was removed from the beaker, wiped with a drying paper and weighted. The weight loss is a measure of the tendency of the binder to “dissolve” in the fuel. It should be pointed out that even if the samples will completely disintegrate after immersion for a sufficiently long time (weight loss 100%), a measurable amount of material (basically asphaltene aggregates) is insoluble and remains suspended or settles on the bottom of the beaker. Moreover, the recorded weights may be slightly in excess, due to kerosene soaking. Nevertheless, the weight loss is a meaningful indicator of the tendency to degrade by the action of the fuel. This test was developed^{37,54–56} while studying fuel resistant binder formulations but can be used as an indirect indicator of the binder structure. This point will be clarified later.

RESULTS AND DISCUSSION

Morphology

BA-SBS. Figure 1 displays the BA and BA-SBS micrographs obtained by POM and FM. In both cases, the white–gray domains correspond to PRP while the darker one to ARP. The FM of BA-SBS shows well-defined polymer-rich islands with

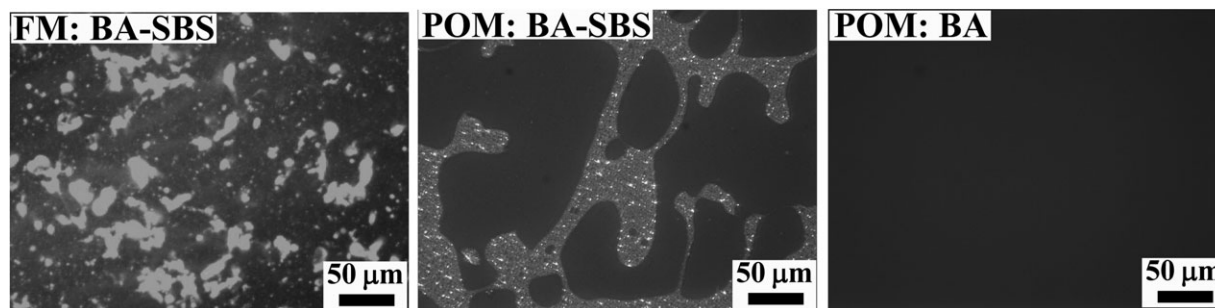


Figure 1. Fluorescence and optical microscopy images of BA and BA-SBS binary blends, showing the presence of wax crystals in PRP (POM of BA-SBS).

irregular shapes and boundaries and of relatively small dimensions which result dispersed in a continuous asphalt matrix. The corresponding image taken by POM appears completely different. To explain such difference, it is necessary to underline that diverse procedures were adopted to prepare the samples. In FM a freeze-fractured surface is observed, while in POM a drop of binder is melted between two glass slices and then cooled down to obtain a thin film.

It is interesting to observe that in PRP, the POM shows a few luminescent points which are neither visible in the asphaltene-rich phase nor in the BA POM image. A possible interpretation is that those points are crystallites of natural waxes formerly present in BA. The selective driving of such waxes into PRP determines both an increased concentration of waxes in such phase and a reduced interaction with asphaltenes which prevalently lies in ARP. Thus, the waxes result able to crystallize in PRP and we have an indication that, even if not compatible with the polymer, the waxes preferentially go in PRP.

Wax M. The micrographs of wax M and binary blend BA-M2 (Figure 2) well identify the evolution of the morphology when the crystallization process shifts from the natural undisturbed conditions (original crystallinity) to the asphaltic environment (residual crystallinity). Wax M alone gives crystallites of big dimensions with morphology typical of a polyethylene based material,⁵⁷ while in the binary BA-M2 mixture the dimension of the crystals is strongly reduced. POM micrographs therefore reveal that M is still able to crystallize within the asphalt but undergoes a remarkable change in shape and dimension of the crystallites. This suggests that M has a certain affinity with the asphalt and therefore partially interacts with some of its compo-

nents. Thanks to its paraffinic structure, M is the wax that mostly should resemble the natural waxes of BA. The morphology of the binary blends suggests that M: (i) partially crystallizes thereby generating its own domains, and (ii) partially interacts with some of the asphalt components, thus modifying the surrounding colloidal environment.

The morphology of the BA-SBS-M ternary blends (Figure 3) introduces further elements of discussion: in the BA-SBS-M2 mixture it is possible to observe wax crystals in both PRP and ARP phases but the concentration of crystals appears to be higher in PRP. This means that M is present in both phases but preferably crystallizes within PRP. Of course, this agrees with POM of BA-SBS which showed the above mentioned light spots (Figure 1).

The same POM micrographs indicate that in ARP the wax crystals are less evident and present a quite reduced spatial distribution. This is consistent with the morphology of the BA-M binary blend and newly suggests that M partially interacts with asphaltenes. These interactions certainly limit the growth of crystallites and probably alter the structural equilibrium of bitumen molecules and molecular segments with expected implications on the bitumen/polymer compatibility.

Accordingly, the FM image in Figure 3 shows morphology considerably different from that of BA-SBS reported in Figure 1. PRP and ARP are still well distinguishable, but PRP appears much more extended and interests almost half of the volume, thus suggesting that the wax may drive into PRP some asphalt components which otherwise will not go there. To confirm this hypothesis, Figure 3 also reports the POM images of the top and bottom fractions obtained after storage at high temperatures. As it would

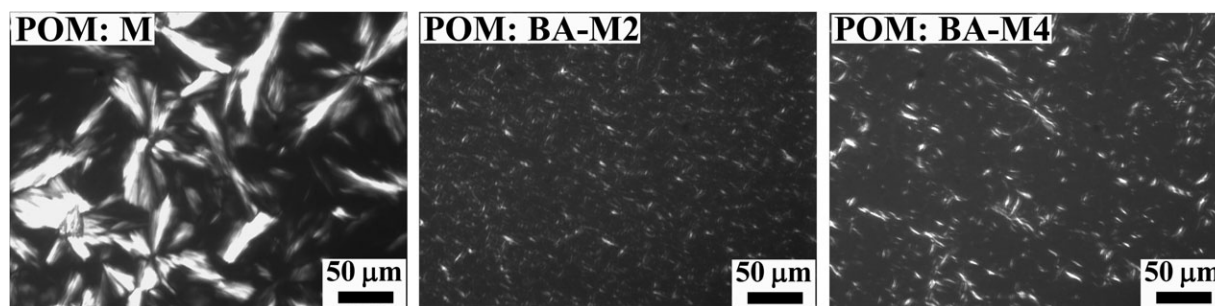


Figure 2. POM images of M and BA-M binary blends, showing the changes of wax morphology after blending with asphalt.

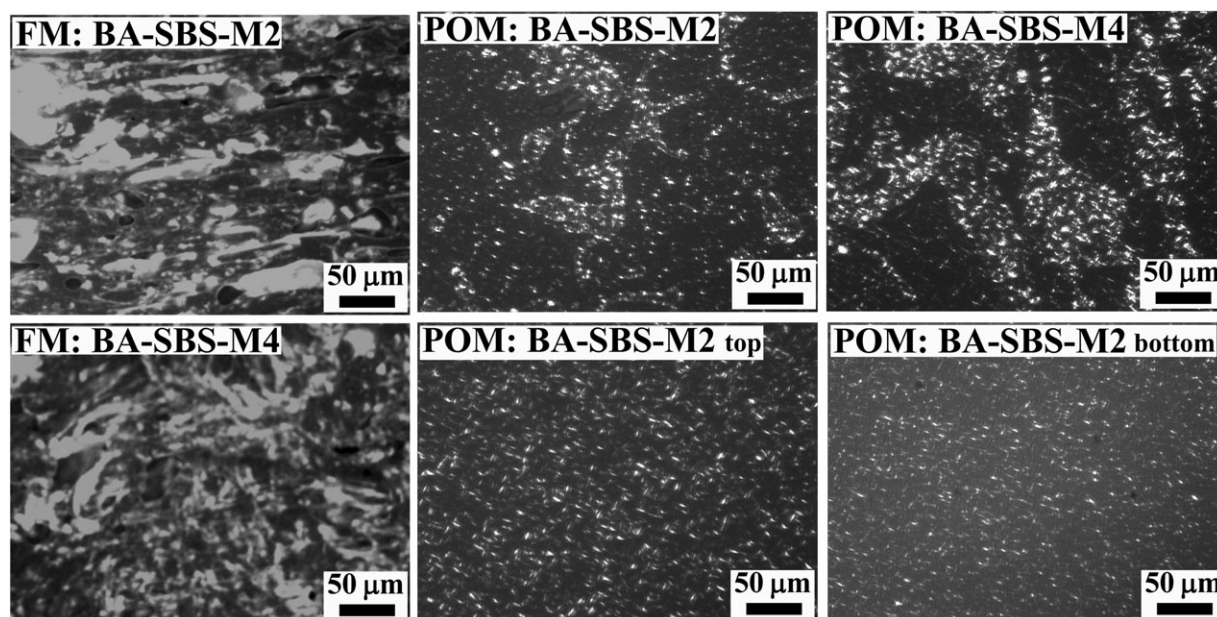


Figure 3. Morphology of BA-SBS-M ternary blends showing the improved compatibility between asphalt and polymer (FM images to be compared with Figure 1) and the prevalence of wax crystals in PRP (POM).

be easily predictable from the FM images, the BA-SBS-M2 mixture is not stable at high temperature storage and PRP migrates to the top of the tube test, while leaving ARP on the bottom. Even if not desirable from an applicative point of view, this instability is helpful to observe the two phases separately and clearly shows that the crystallites are more concentrated in the top section. So, the part of M which interacts with bitumen favors the asphalt migration into the swelled polymeric phase and basically generates a change in the overall compatibility between asphalt and polymer. It is worth nothing that after the phase separation all the domain features for the ternary systems disappear in the POM images taken at the top and bottom and this denotes a very low compatibility between the chosen asphalt and polymer. A similar behavior was observed also for the other two waxes.

Wax PEox. The POM images (Figure 4) indicate that in BA-PEox2 no wax crystals are visible, while a diffuse presence of small crystals (considerably smaller than those of the pure wax) can be appreciated in BA-PEox4. This suggests that the behavior of PEox is quite similar to that of M, being the former less prone to crystallize and thus probably more prone to interact

with asphalt molecules. This is not surprising and can be directly ascribed to the specific chemical nature of this wax. In a partially oxidized polyethylene, the polar functional groups disturb the crystallization process because (i) they introduce irregularity in the chain and (ii) they can interact with resins and asphaltenes.

Figure 5 reports the morphologies of asphalt-SBS-PEox ternary blends.

The first important observation deals with the swelling dynamics and the overall equilibrium between ARP and PRP. Compared with BA-SBS-M2, the result is a less swelled PRP phase, as it is confirmed by FM which shows gray island of bigger dimension and smoother boundaries.¹⁷ Hence, contrary to M, PEox hinders the mechanism of migration of the lighter and less polar asphalt fractions thus limiting the compatibility between asphalt and polymer.

The interpretation of such morphologies is different from that of the previous case, because the functionalized wax is more prone to interact with ARP.¹⁸ Therefore, the most probable indication is that PEox probably goes preferentially in ARP, where,

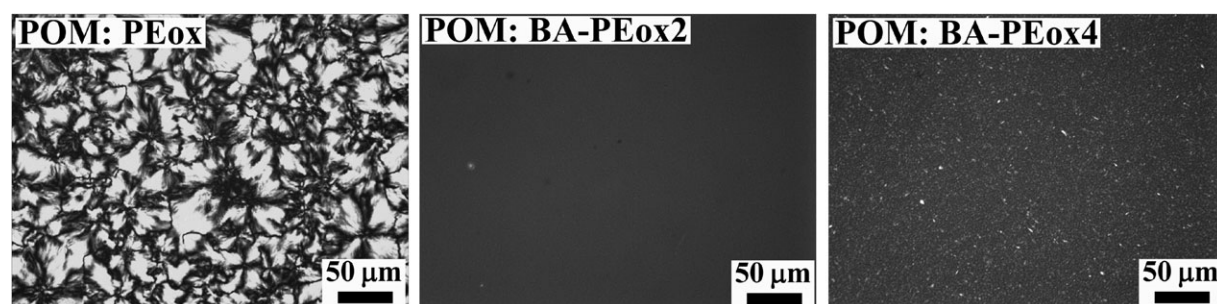


Figure 4. POM images of PEox and BA-PEox binary blends, showing that PEox is hardly able to crystallize, after blending with BA.

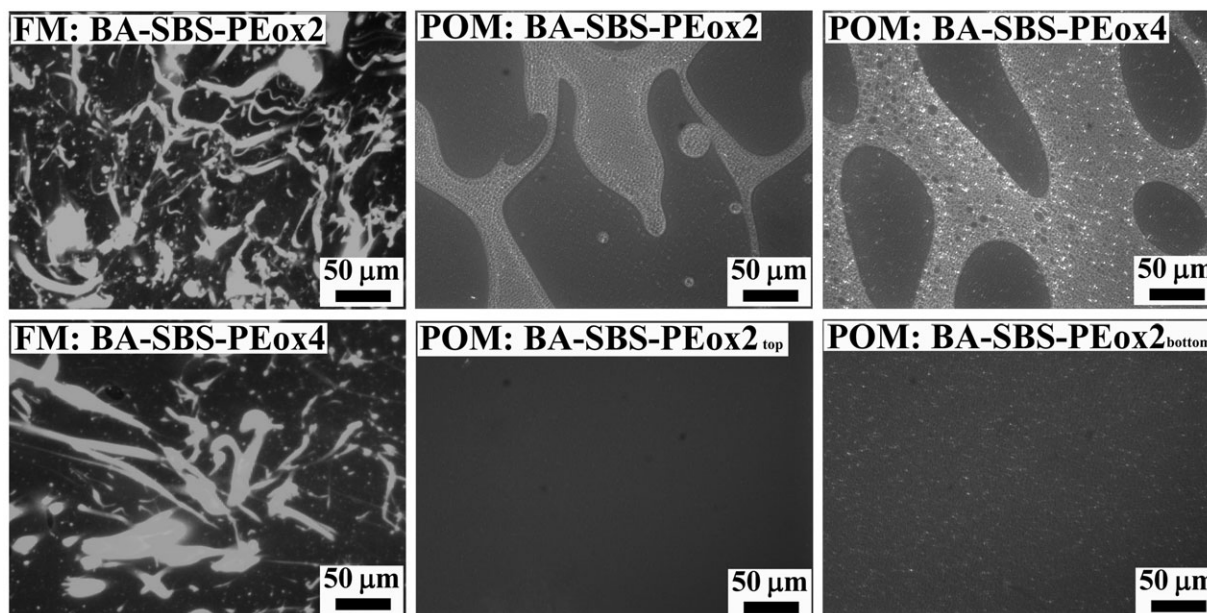


Figure 5. Fluorescence and optical microscopy images of BA-SBS-PEox ternary blends, showing the reduced compatibility between asphalt and polymer (FM images to be compared with Figure 1) and the tendency of PEox to go in ARP (POM).

thanks to its paraffinic part, strongly interacts and drives also part of the less polar asphalt molecules. It is important to observe that even if prevalently localized in ARP, the PEox wax is not able to crystallize in such phase (see POM image of BA-SBS-PEox2 in Figure 5). With 4.0% PEox, the wax concentration is high enough to have crystals in both ARP and PRP (see POM images in Figure 5). Note that in the POM image of BA-SBS-PEox4, the crystals are more evident in PRP where there is a lower concentration of components able to interact with PEox, so that the wax may give much regular crystals in such phase. This is confirmed by the POM images of the top and bottom of BA-SBS-PEox2 mixture, which shows some crystals only in the bottom. Hence, PEox preferably resides within ARP but is hardly able to crystallize in this phase. In addition, contrary to what found for M, this process does not positively affect the asphalt/polymer compatibility.

Wax PPMA. PPMA has a different behavior if compared with the other two waxes (Figure 6). In both BA-PPMA2 and BA-PPMA4 mixtures, the crystallites appear similar in structure and dimension to those of the pure wax. PPMA forms big

crystallites which correspond to a large dimension network and this peculiar behavior suggests that PPMA is unable to create intimate interactions with the asphalt components. In other words, PPMA appears as almost completely incompatible with BA. Of course, this incompatibility may be ascribed to the propylene backbone. Indeed, there are also the maleic functionalities which may be able to interact with resins and asphaltenes. Nevertheless, considering the dimension of the crystals, such interactions are weak, or at least weaker than those among wax molecules.

To investigate the overall phase equilibrium in PPMA-based ternary blends, we start from FM (Figure 7). FM indicates that PRP and ARP are almost equivalent in extension and PRP is uniformly distributed and made of small, irregular and interconnected domains. The FM picture therefore indicates an asphalt/polymer compatibilizing effect. This is quite surprising considering the supposed absence of interactions between asphalt and wax. On the other side, it is also well known that maleic functionalities may interact with asphalt and also exert an asphalt/polymer compatibilizing effect^{58–65} which is probably

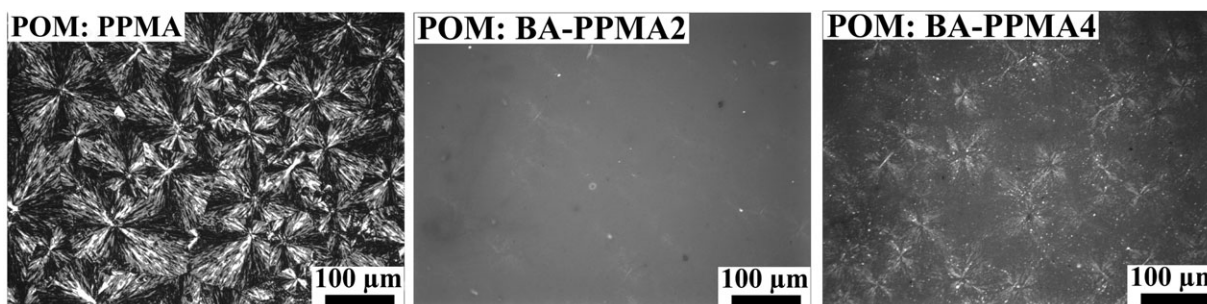


Figure 6. POM images of PPMA and BA-PPMA binary blends, showing that, contrary to the other waxes, the wax crystals in the binary blends have dimension comparable with those of pure wax.

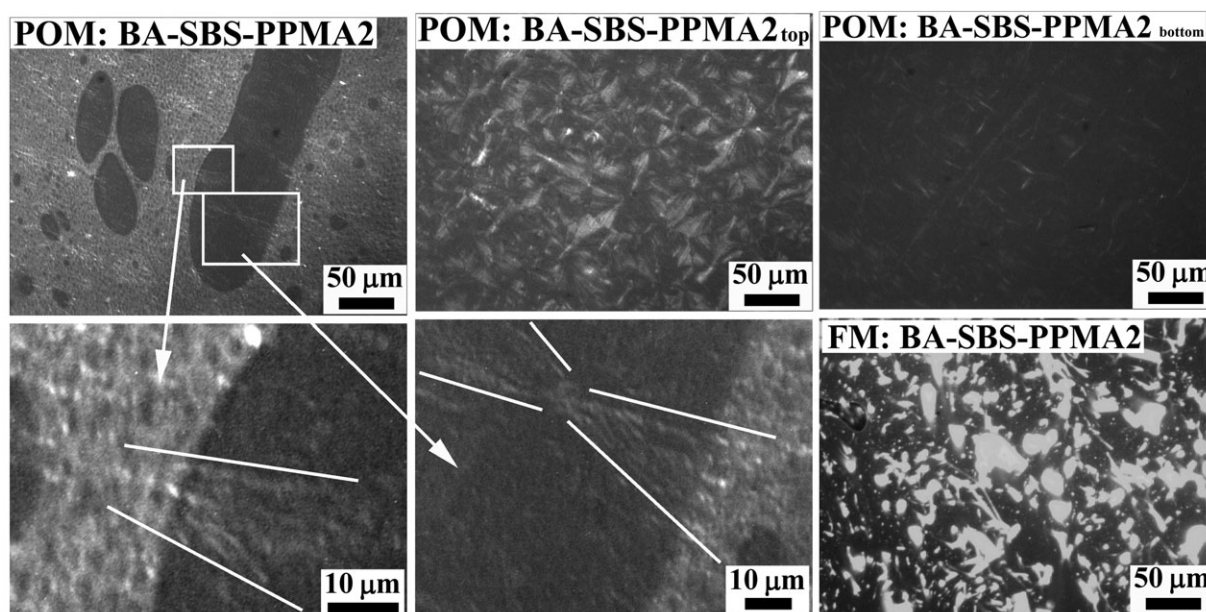


Figure 7. Fluorescence and optical microscopy images of BA-SBS-PPMA ternary blends, showing the improved compatibility between asphalt and polymer (FM images to be compared with Figure 1). In the POM enlargements, some big wax crystals can be seen across the PRP and ARP phases.

the main responsible for the obtained morphology. The POM images indicate that the crystals are present in both PRP and ARP phases. Moreover, thanks to their big dimensions, it can be appreciated that the crystallites cross-over the two phases (see enlarged area in the figure, where the crystallites boundaries are highlighted with a white line). Therefore, from these images, it is not clear if PPMA locate preferentially in PRP or ARP.

We can summarize what has been found for each of the waxes with the following points:

- In the binary BA-SBS blend, natural waxes (even if not compatible with the polymer) preferentially go in PRP.
- In the ternary blends, wax M preferentially crystallizes within PRP where it drives the less polar bitumen components, thus slightly enhancing the compatibility with the polymer.
- PEox limits the migration of the lighter and less polar asphalt fractions thus reducing the compatibility between asphalt and polymer; in the ternary blends PEox is prevalently localized in ARP.
- PPMA appears as almost completely incompatible with BA, but behaves as an asphalt-polymer compatibilizer; in the ternary blends it is not clear if PPMA locate preferentially in PRP or in ARP.

Differential Scanning Calorimetry

Table II summarizes the results of the DSC analysis of BA, BA-SBS, ternary blends with 2.0% wax and their respective top and bottom fractions. The table reports glass transition temperatures (T_{g1} and T_{g2}) of the mixes, as well as the melting temperatures (T_m) and enthalpies (ΔH_m) of the added waxes. The last column is calculated by normalizing the wax melting enthalpy based on wax content and then expressing this value as a percentage of

the melting enthalpy observed for the pure wax. Therefore this column basically represents the residual crystallinity of the waxes in the binary and ternary blends and quantifies the percentage of wax that crystallizes after blending. The residual crystallinity has been also determined for the top and bottom fractions obtained after storage tests of the ternary blends. These data can provide information about wax distribution between PRP (top) and ARP (bottom) fractions. However, it should be pointed out that the melting enthalpy just represent the content of crystalline wax and its numerical value is not simply proportional to the amount of wax, but it also depends on the ability of the wax to crystallize in the matrix where it is dispersed. Of course, this ability can be different between PRP or ARP which may contain different amounts of amorphous wax. Therefore, the reported data represent the total amount of crystalline wax, which can be different from the total amount of wax.

The first interesting observation is related to the residual crystallinity in the binary blends, which results very low for M, intermediate for PEox and high for PPMA. The residual crystallinity can be somehow interpreted as a measure of the interactions between the wax and the base asphalt. A low crystallinity may indicate a high degree of interactions, which disturb the crystal grow and regularity, while a high crystallinity indicates a low degree of interactions. The obtained values are in agreement with the observations made through microscopy. PPMA does not interact significantly with asphalt and give rise to the formation of crystals almost identical to those formed when not mixed. Among M and PEox, it seems that the former is the one mostly influenced by the interactions with asphalt molecules. This result is somehow in contradiction with a previous one,⁵³ where it was found that the same wax had a residual crystallinity of 57% when mixed with similar asphalt. However, in that case the mix contained 6% of wax and this difference in

Table II. Results of DSC Analyses

	T_{g1} (°C)	T_{g2} (°C)	T_m (°C)	ΔH_m (J g ⁻¹)	Cryst. ^a (%)
BA	-16.6	20.9	-	-	-
BA-SBS	-13.4	23.7	-	-	-
BA-SBS Bottom	-14.2	25	-	-	-
BA-SBS Top	-12.2	-	-	-	-
M	-	-	105.7	220.4	-
BA-M2	-14.7	24.5	110.1	0.9	21
BA-SBS-M2	-13.7	25.4	110.7	1.3	31.5
BA-SBS-M2 Bottom	-16.6	25.5	111.0	1.1	26.6
BA-SBSM2 Top	-14.9	23.2	106.3	1.7	41.3
PPMA	-16.6	-	157.5	80.3	-
BA-PPMA2	-14.3	25.6	151.9	0.8	50.8
BA-SBS-PPMA2	-13.9	25.8	154.6	1.0	66.6
BA-SBSPPMA2 Bottom	-13.7	28.5	150.0	0.7	46.6
BA-SBS-PPMA2 Top	-14.1	24.6	146.6	1.1	73.3
PEox	-13.8	-	111.2	137.5	-
BA-PEox2	-13.6	-	97.8	1.55	57.5
BA-SBS+PEox2	-13.6	-	98.1	1.8	70.0
BA-SBS-PEox2 Bottom	-14.7	-	98.0	2.45	95.3
BA-SBS-PEox2 Top	-14.4	-	98.1	1.7	66.1

^aCalculated as $\frac{\Delta H_m}{\Delta H_m(\text{pure wax})} \frac{(W_w + W_{BA} + W_{SBS})}{W_w} \times 100$, where W_w , W_{BA} , and W_{SBS} are the percentage weight content of wax, BA, and SBS, respectively.

the content can easily explain the difference. The total amount of wax that interacts with the asphalt components is relatively limited and it is almost independent from the wax content. Therefore, for high wax contents, the percentage of wax involved in such interactions results much lower and the residual crystallinity is high.

Going to the ternary mixes, in all cases, the residual crystallinity was found to be higher than that of the binary ones. This may

suggest that the interactions established between asphalt and polymer may compete with those between wax and asphalt, thus increasing the wax molecules able to participate to the crystallization process.

Further indications are provided by the analysis of ΔH_m in the top and bottom fractions derived from the storage stability test, which are also in agreement with the supposition made from the morphological analysis. M and PPMA reside preferably in

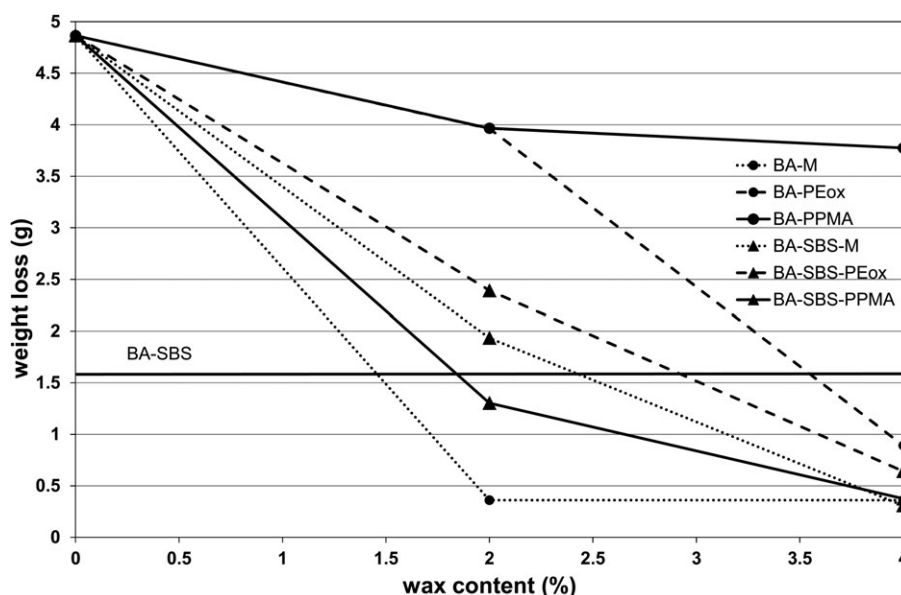


Figure 8. Solubility of the mixtures in kerosene jet fuel A1.

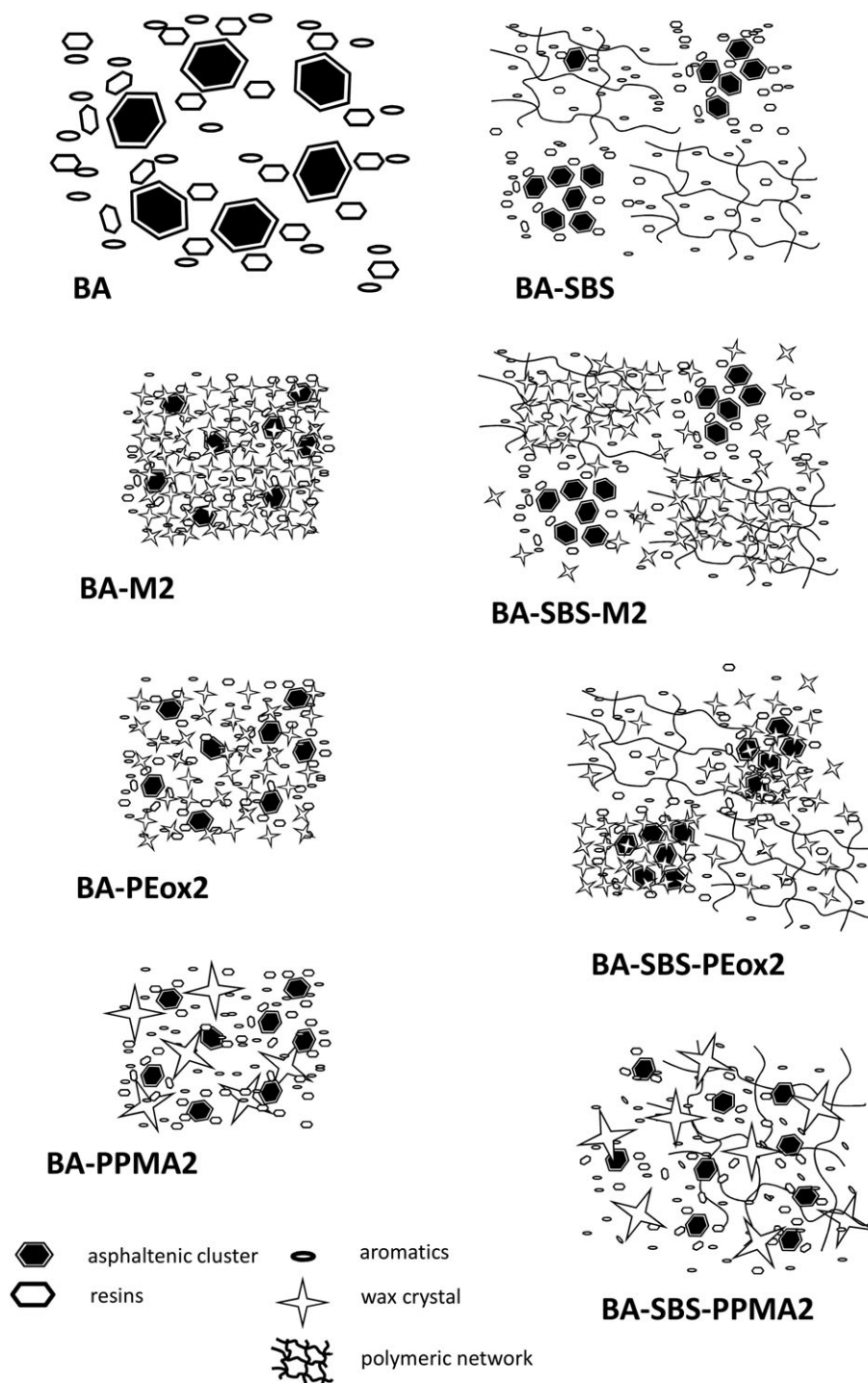


Figure 9. Hypothetical structure of BA, binary and ternary blends.

the top fraction (PRP), while PEox in the bottom fraction (ARP).

The final concern is to investigate if the data provided by DSC analysis related to the asphalt glass transitions can give a further validation to the discussion relative to the role of polymer and waxes. The presence of two separated glass transitions in BA is well known and was interpreted as due to a separation of the aliphatic and aromatic compounds during cooling.⁶⁶ The sepa-

ration is not complete due to the high viscosity at low temperatures and therefore the upper glass transition (T_{g2}) derives from the material enriched in paraffinic fraction, while the lower (T_{g1}) from the material depleted of paraffines. As a general observation, in all the mixtures there is a detectable increase in both glass transitions. This is reasonably due to the interactions with the polymer and/or waxes, which limits the mobility of the interested fractions. The magnitude of such variation is related

with the degree of interaction. However, due to the low content of waxes there is an intrinsic difficulty in the evaluation of the glass transition. The values reported in the table (obtained as a mean of four to five different measurements) are affected by an uncertainty of about 0.5–1.5°C, which do not allow to hazard a deeper discussion in this sense.

Solubility Tests

The results of the solubility tests are reported in Figure 8 where the weight loss after 2 h of immersion in jet fuel A-1 is reported as a function of the wax content. The horizontal line represents the weight loss of the binary BA-SBS mixture, while the point on the vertical axis represents the weight loss of BA alone.

Before commenting this graph, it is necessary to briefly explain the meaning of the test. The contribution of different modifiers on the fuel resistance of bituminous binders was deeply analyzed in previous works where three classes of modifiers were considered: polymers, waxes and ground tire rubber.^{37,54–56} In those works the “fuel resistance” was intended as a reduced solubility of an asphaltic binder in conventional fuels. Being the tests mainly performed by using a kerosene jet fuel, this is also referred as an “anti-kerosene” effect. The solubility tests showed that all the above mentioned modifiers can increase the resistance to fuel, being different the mechanism of the anti-kerosene effect. Moreover, important differences were recorded between the three classes of modifiers and the different types of modifiers in each class. Polymers may lead to a quite sensible improvement, being the final fuel-resistance strongly dependent on the polymer structure and compatibility with bitumen. Waxes generally produce the most important improvement in the fuel resistance. With regard to the mechanisms involved in improving fuel resistance, the reduced solubility obtained with polymers is due to a selective swelling which involves the bitumen components that are more soluble in kerosene. In other words, saturates and aromatics, which are more soluble in kerosene, result less accessible to the fuel being entrapped in the polymeric network (which means in PRP). In contrast, the waxes form a physical barrier composed of a network of insoluble crystals well dispersed in the whole bituminous mass. Thus: (i) a polymer has a good antikerosene effect when it is highly compatible with the asphalt and able to swell the more soluble asphalt fractions, while (ii) a wax has a good antikerosene effect when able to form a network of small interconnected crystal uniformly distributed in the asphalt matrix, which acts as a shield for the fuel molecules. The latter point was confirmed by evaluating the effect of wax concentration on the fuel resistance.⁵⁶ It was found that for an amidic wax there was a sort of critical concentration corresponding to an abrupt change in the recorded values of the solubility. For wax content lower or equal to 0.9% by weight, the samples completely dissolved after 2 h of immersion. Passing from 0.9 to 1.0% of wax, the weight loss resulted about 33%, while higher concentrations of wax did not significantly change the solubility. Such big changes showed that 1.0% of wax corresponded to a situation where the crystal network reaches a sort of continuity, somehow analogous to the phase inversion of PMAs, which induces a macroscopic effect on the binder properties.

Therefore, even if the fuel resistance is out of the scope of this article, it can be used as an indirect indicator of the binder structures and can give some suggestions relative to how and how much polymer and wax do interact one to each other thus altering the blend structure.

BA-SBS. The solubility is more than halved by the polymer addition. Having in mind the supposed mechanism for such anti-kerosene effect, we can say that the most soluble asphalt components are driven into PRP thus resulting less accessible to the solvent.

Wax M. The Montan wax M in the binary mixtures with BA determines a strong reduction of the solubility, independently on its concentration. This means that the above mentioned critical concentration for M is lower than 2.0%. The used concentrations guarantee the presence of a wax network well-structured and distributed in BA. On the other hand, the morphology showed that in the binary BA-M2 mixture the dimension of the crystals results strongly reduced due to the interactions with the asphalt components (this reduction is helpful in terms of anti-kerosene effect, because it leads to a more structured network). However, quite surprisingly, in the ternary BA-SBS-M2 mixture the solubility is almost identical to that of the BA-SBS mixture, thus considerably higher than what obtained with M alone. This can be explained in accordance with the observation made by POM (Figures 2 and 3). In the BA-SBS-M mixture, M behaves like the paraffines already present in the asphalt (and similar in chemical structure) and preferentially goes in PRP. This determines a reduced concentration of wax in ARP where probably the crystals content results lower than the critical one. As a consequence, the antikerosene effect remains limited to the PRP and results equivalent to that of the BA-SBS mixture.

Wax PEox. From Figure 8, we have the indication that in the binary mixtures, differently from M, a 2.0% concentration is not enough to form the barrier-network which appears at 4.0%. Again, this well agrees with the results of morphological analyses. As it was already observed, in a partially oxidized polyethylene the functional groups introduce irregularity in the chain and interact with resins and asphaltenes, thereby disturbing the crystallization process. The POM images confirm that in BA-PEox2 no wax crystals are visible, while a diffuse presence of small crystals (considerably smaller than those of the pure wax) can be appreciated in BA-PEox4 (Figure 4). The ternary mixtures gave a result similar to what previously found for wax M. However, in this case the mixtures with only 2.0% of PEox show a resistance to the solvent which is even lower than that of BA-SBS. The interpretation is different than that of the previous case, because the functionalized wax interacts with ARP. However, even if prevalently localized in ARP, the PEox wax is not able to crystallize in such phase (see POM image of BA-SBS-PEox2 in Figure 5) and there are more soluble molecules in this kerosene “unshielded” phase, thus explaining the high solubility of BA-SBS-PEox2. In BA-SBS-PEox4, the wax concentration is high enough to have crystals in both ARP and PRP and thus we have a good solvent resistance.

Wax PPMA. As in the previous cases, for PPMA the first interesting information comes from the solubility of the binary mixtures: even at 4.0% concentration, PPMA does not significantly enhance the solvent resistance. This is not due to absence of wax crystals, but to the nature of the crystals. Once again, we have a confirmation in the morphologies of the mixtures. As clearly displayed by Figure 6, the wax crystallites are almost equal in structure and dimension to those of the pure wax. So, PPMA generates a large dimension network unable to exert a good shield action. However, in the ternary mixture PPMA is the only one which at 2.0% concentration gives solubility lower than that of the BA-SBS binary mixture. This cannot be interpreted as a simple additive (wax plus polymer) effect, but appears to be a synergistic one. The morphology of such mixtures showed the enhanced asphalt/polymer compatibility and thus clearly demonstrated that a higher percentage of asphalt components are driven in the swelled PRP, thus becoming unavailable or less accessible to solvent molecules. In this case the antikerosene effect comes from the polymer and not from the wax network. However, the wax indirectly participates by increasing the polymer swelling.

The solubility tests basically confirm all the hypothesis deduced from the morphological analysis. Therefore, we can rewrite the points already summarized at the end of the “Morphology” section, from a “solubility” point of view.

- In the binary BA-SBS blend, natural waxes and the other most soluble asphalt components preferentially go in PRP.
- The wax M in the binary mixtures with BA determines a strong reduction of the solubility by creating a crystals network. However, in the BA-SBS-M mixture, M behaves like the natural waxes (similar in chemical structure) and preferentially goes in PRP, so that the network is not present and the antikerosene effect is lost.
- The functional groups of PEox interact with resins and asphaltenes, thereby disturbing the crystallization process. Therefore, differently from M, PEox does not alter the solubility in the binary mixtures. At the same time, in the ternary mixture PEox limits the antikerosene effect of the polymer because it keeps the apolar molecules in ARP.
- The low interactions of PPMA with BA allow the wax to form big crystals which do not influence the solubility. On the contrary, even if the dimension of the crystals remains unchanged, in the ternary mixtures PPMA gives a solubility lower than that of the BA-SBS binary mixture. This means that the anti-kerosene effect comes from the polymer and confirms the increased BA-SBS compatibility: there is a higher percentage of asphalt components in PRP which is less accessible to solvent molecules.

A Structural Model

To summarize and better visualize the hypothesized colloidal structures of the mixtures, Figure 9 is built in similarity with the scheme proposed by Pfeiffer and Saal.⁶⁷

In the base asphalt some asphaltenic clusters are associated together to form irregular open packed micelles which are peptized by resins. When the base asphalt is modified with SBS (BA-SBS), the asphaltenic micelles due to their dimension and

polar character are not able to swell the polymeric network, thus giving rise to the formation of well separated PRP and ARP domains.

For the binary and ternary mixtures containing the three waxes, there are as many different structures. In BA-M2 there are small crystallites forming an interconnected network uniformly distributed in the blend. When SBS is added, the nature of the mixture is again biphasic, being the wax crystallites more concentrated in PRP and partially disjointed in ARP.

The binary mixture BA-PEox2 has a structure similar to BA-M2, being the main difference the absence of the wax network: the crystallites are still of small dimensions, but not close enough to be interconnected (no shield effect). In contrast, BA-SBS-PEox behaves quite opposite to BA-SBS-M2. Again there are two distinct phases, but the wax crystallites are mainly located in ARP.

Finally, BA-PPMA2 has large isolated wax crystallites, absolutely unable to block the solvent molecules. In the ternary blend, wax crystallites are located in both PRP and ARP, but the main effect of wax is the higher asphalt/polymer compatibility which leads to a highly swelled polymeric network able to include almost all the asphalt components. Nevertheless, the presence of PRP and ARP separate domains is still detectable.

CONCLUSIONS

This preliminary investigation on potential WMPMA based on the use of waxes indicates how the chemical nature of the wax may influence the whole binder structure. Depending on their chemical composition, the waxes preferentially interact with different asphalt components and may or not interact also with the polymer. Such information can be obtained by a simple morphological analysis which highlights the presence, position and dimension of wax crystals, as well as the shape and dimensions of the polymer-rich and asphaltene-rich phases. The tendency of these two phases to separate during storage at high temperature, revealed to be a valid help to visualize both of them.

The behavior of the asphalt/polymer/wax ternary systems cannot be predicted from a simple additive rule derived from the asphalt/wax and asphalt/polymer binary systems. The complex interactions among the three ingredients may lead to completely different structures depending on the wax characteristics. Of course, this will directly influence the “warm” effect and also the final properties of the binder, from its storage stability to the in service properties. The latter point is under investigation and will be the subject of future publications. Nevertheless, the solubility of the binders in a kerosene jet fuel gave a first indication of the different properties deriving from different waxes and gave also an indirect confirmation of the internal structures hypothesized from the morphological and calorimetric analysis.

REFERENCES

1. Federal Highway Administration, Warm-Mix Asphalt. Available at: <http://www.fhwa.dot.gov/pavement/asphalt/wma.cfm> (accessed January 10, 2013).

2. Lesueur, D. *Adv. Colloid Interface Sci.* **2009**, *145*, 42.
3. Edwards, Y.; Redelius, P. *Energy Fuels* **2003**, *17*, 511.
4. Edwards, Y.; Isacson, U. *Road Mater. Pavement Des.* **2005**, *6*, 281.
5. Edwards, Y.; Isacson, U. *Road Mater. Pavement Des.* **2005**, *6*, 439.
6. Warth, A. B. *The Chemistry and Technology of Waxes*; Reinhold: New Jersey, **1956**.
7. Thanh, N. X.; Hsieh, M.; Philp, R. P. *Org. Geochem.* **1999**, *30*, 119.
8. Lu, X.; Kalman, B.; Redelius, P. *Fuel* **2008**, *87*, 1543.
9. Lu, X.; Langton, M.; Olofsson, P.; Redelius, P. *J. Mater. Sci.* **2005**, *40*, 1893.
10. Michon, L. C.; Netzel, D. A.; Turner, T. F.; Martin, D.; Planche, J. P. *Energy Fuels* **1999**, *13*, 602.
11. Lu, X.; Redelius, P. *Energy Fuels* **2006**, *20*, 653.
12. Lu, X.; Redelius, P. *Construct. Build. Mater.* **2007**, *21*, 1961.
13. Lee, H.; Wong, W. *Construct. Build. Mater.* **2009**, *23*, 507.
14. Wong, W.; Li, G. *Construct. Build. Mater.* **2009**, *23*, 2504.
15. Giuliani, F.; Merusi, F. *Int. J. Pavement Res. Technol.* **2009**, *2*, 51.
16. Merusi, F.; Caruso, A.; Roncella, R.; Giuliani, F. *Transport. Res. Rec.* **2010**, *2180*, 110.
17. Merusi, F.; Giuliani, F. *Mater. Struct.* **2011**, *44*, 1809.
18. Polacco, G.; Stastna, J.; Biondi, D.; Zanzotto, L. *Curr. Opin. Colloid Interface Sci.* **2006**, *11*, 230.
19. Edwards, Y.; Tasdemir, Y.; Butt, A. A. *Mater. Struct.* **2010**, *43*, 123.
20. Kim, H.; Lee, S.-J.; Amirhanian, S. N.; Park, T.-S. *J. Test. Eval.* **2011**, *39*, 728.
21. Kim, H.; Lee, S.-J.; Amirhanian, S. N. *Can. J. Civil Eng.* **2010**, *37*, 17.
22. Huang, Y. C.; He, Z. Y. *Appl. Mech. Mater.* **2011**, *97*, 367.
23. Cao, W.-D.; Liu, S.-T.; Cui, X.-Z. *Appl. Mech. Mater.* **2011**, *99*, 875.
24. Akisetty, C. K.; Lee, S.-J.; Amirhanian, S. N. *Int. J. Pavement Eng.* **2010**, *11*, 153.
25. Mallick, R. B.; Bradley, J. E.; Bradbury, R. L. *Transport. Res. Rec.* **2007**, *1998*, 112.
26. Xiao, F.; Zhao, W.; Amirhanian, S. N. *J. Test. Eval.* **2011**, *39*, 290.
27. Gonzalez, V.; Martinez-Boza, F. J.; Navarro, F. J.; Gallegos, C.; Perez-Lepe, A.; Paez, A. *Fuel Process. Technol.* **2010**, *91*, 1033.
28. Yero, A. S.; Hainin, M. R. *Int. J. Res. Rev. Appl. Sci.* **2011**, *8*, 171.
29. Akisetty, C. K.; Gandhi, T.; Lee, S.-J.; Amirhanian, S. N. *Can. J. Civil Eng.* **2010**, *37*, 763.
30. Becker, I. M.; Muller, A. J.; Rodriguez, Y. *J. Appl. Polym. Sci.* **2003**, *90*, 1772.
31. Airey, G. D. *J. Mater. Sci.* **2004**, *39*, 951.
32. Fawcett, A. H.; McNelly, T. *Polym. Eng. Sci.* **2001**, *41*, 1251.
33. Fawcett, A. H.; McNelly, T. *Colloid Polym. Sci.* **2003**, *281*, 203.
34. Lu, X.; Isacson, U. *J. Appl. Polym. Sci.* **2000**, *76*, 1811.
35. Fawcett, A. H.; McNelly, T. *Polymer* **2000**, *41*, 5315.
36. Airey, G. D. *Construct. Build. Mater.* **2002**, *16*, 473.
37. Giuliani, F.; Merusi, F.; Filippi, S.; Biondi, D.; Finocchiaro, M. L.; Polacco, G. *Fuel* **2009**, *88*, 1539.
38. Polacco, G.; Stastna, J.; Biondi, D.; Antonelli, F.; Vlachovicova, Z.; Zanzotto, L. *J. Colloid Interface Sci.* **2004**, *280*, 366.
39. Selvavathi, V.; Sekar, V. A.; Sriram, V.; Sairam, B. *Petroleum Sci. Technol.* **2002**, *20*, 535.
40. Spontak, R. J.; Patel, N. P. In *Developments in Block Copolymer Science and Technology*; Hamley, I. W., Ed.; Wiley: New York, **2004**; Chapter 5, p 159.
41. Yang, X.; Kilpatrick, P. *Energy Fuels* **2005**, *19*, 1360.
42. Fuhr, B. J.; Cathrea, C.; Coates, L.; Kalra, H.; Majeed, A. I. *Fuel* **1991**, *70*, 1293.
43. Carbognani, L.; Orea, M.; Fonseca, M. *Energy Fuels* **1999**, *13*, 351.
44. Garcia, M. D. C. *Energy Fuels* **2000**, *14*, 1043.
45. Mahmoud, R.; Gierycz, P.; Solimando, R.; Rogalski M. *Energy Fuels* **2005**, *19*, 2474.
46. Carbognani, L.; De Lima, L.; Orea, M.; Ehrmann, U. *Pet. Sci. Technol.* **2000**, *18*, 607.
47. Tinsley, J. F.; Jahnke, J. P.; Dettman, H. D.; Prud'home, R. K. *Energy Fuels* **2009**, *23*, 2056.
48. Tinsley, J. F.; Jahnke, J. P.; Adamson, D. H.; Guo, X.; Amin, D.; Kriegel, R.; Saini R.; Dettman, H. D.; Prud'home, R. K. *Energy Fuels* **2009**, *23*, 2065.
49. Ashbaugh, H. S.; Guo, X. H.; Schwahn, D.; Prud'homme, R. K.; Richter, D.; Fetters, L. J. *Energy Fuels* **2005**, *19*, 138.
50. Ronningsen, H. P.; Bjorndal, B.; Hansen, A. B.; Pedersen, W. B. *Energy Fuels* **1991**, *5*, 895.
51. Holder, G. A.; Winkler, J. *Nature* **1965**, *207*, 719.
52. Radulescu, A.; Fetters, L. J.; Richter, D. *Adv. Polym. Sci.* **2008**, *210*, 1.
53. Polacco, G.; Filippi, S.; Paci, M.; Giuliani, F.; Merusi, F. *Fuel* **2011**, *95*, 407.
54. Merusi, F.; Polacco, G.; Nicoletti, A.; Giuliani, F. *Mater Struct* **2010**, *43*, 1271.
55. Merusi, F.; Giuliani, F.; Filippi, S.; Moggi, P.; Polacco, G. *J. Transport. Eng.* **2011**, *137*, 874.
56. Polacco, G.; Filippi, S.; Paci, M.; Markanday, S.; Merusi, F.; Giuliani, F. In *Polymer Modified Bitumen: Properties and Characterisation*; MacNally, T., Ed.; Woodhead Publishing in Materials: Oxford, **2011**; Chapter 11, p 336.
57. Kitamaru, R. *Adv. Polym. Sci.* **1998**, *137*, 41.
58. Vargas, M. A.; Manero, O. *J. Appl. Polym. Sci.* **2011**, *119*, 2422.
59. Kang, Y.; Wang, F.; Chen, Z. *Chem. Eng. J.* **2010**, *164*, 230.
60. Yeh, P. H.; Nien, Y. H.; Chen, W. C.; Liu, W. T. *Polym. Compos.* **2010**, *31*, 1738.

61. Vargas, M. A.; Lopez, N. N.; Cruz, M. J.; Calderas, F.; Manero, O. *Rubber Chem Technol* **2009**, *82*, 244.
62. Yeh, P. H.; Nien, Y. H.; Chen, J. H.; Chen, W. C.; Chen, J. S. *Polym. Eng. Sci.* **2005**, *45*, 1152.
63. Becker, Y. M.; Mueller, A. J.; Rodriguez, Y. J. *Appl. Polym. Sci.* **2003**, *90*, 1772.
64. Kumari, D.; Chollar, B. H.; Zenewitz, J. A.; Boone, J. G. Preprints– *Am. Chem. Soc. Div. Petroleum Chem.* **1990**, *35*, 531.
65. Nadkarni, V. M.; Shenoy, A. V.; Mathew, J. *Indus. Eng. Chem. Product Res. Dev.* **1985**, *24*, 478.
66. Chambrion, P.; Bertau, R.; Ehrburger, P. *Fuel* **1996**, *75*, 144.
67. Pfeiffer, J. P.; Saal, R. N. J. *J. Phys. Chem.* **1940**, *44*, 139.